38th ERF, September 3–6, 2013, Moscow, Russia

097

Experimental Investigation of Perpendicular Vortex Interaction over an Oscillating Airfoil in Dynamic Stall Conditions

A. Zanotti*, G. Gibertini and A. Mencarelli

Politecnico di Milano – Dipartimento di Scienze e Tecnologie Aerospaziali

Via La Masa 34, 20156 Milano – Italy

e–mail: *alex.zanotti@polimi.it

Keywords: Vortex Interaction, Oscillating airfoil, PIV, Hot-Wire Anemometry.

Abstract

An experiment of perpendicular Blade Vortex Interaction with an oscillating airfoil model has been set up and carried out. The use of the Particle Image Velocimetry allowed to see very interesting effects of the vortex induction. In particular, the combined effect of the vortex induction with the airfoil oscillation produces, in some conditions, a wide flow separation. This experiment indicates that also a perpendicular vortex can remarkably perturb the struck blade.

Nomenclature

BVI	Blade Vortex Interaction
c	blade section model chord [m]
C_L	lift coefficient
DSTA	Dipartimento di Scienze e Tecnologie Aerospaziali
f	oscillation frequency [Hz]
HW	Hot-Wire
k	reduced frequency, $= \pi f c/U_\infty$
Ma	Mach number
PIV	Particle Image Velocimetry
Re	Reynolds number, $\equiv cU_\infty/\nu$
$\lvert U \rvert$	velocity magnitude [m/s]
U_∞	free-stream velocity [m/s]
u	stream-wise velocity component [m/s]
v	span-wise velocity component [m/s]
w	vertical velocity component [m/s]
VG	Upstream Model
x	stream-wise coordinate [mm]
y	span-wise coordinate [mm]
z	vertical coordinate [mm]
y_v	vortex core centre span-wise coordinate [mm]
z_v	vortex core centre vertical coordinate [mm]
α	angle of attack [deg]
α_m	mean angle of attack [deg]
α_a	pitching oscillation amplitude [deg]
ν	cinematic viscosity of air [m^2/s]

1 Introduction

The Blade Vortex Interaction (BVI) [1, 2] on the helicopter rotor represents one of the most investigated topics in rotorcraft aerodynamics due to its implications on noise and vibrations. Therefore, experiments that allow to investigate any physical phenomenon related to BVI are interesting and can help the effort to find ways to reduce its unwanted effects.

This paper describes an exeperiment of perpendicular Blade Vortex Interaction[3, 4] with an oscillating airfoil model that has been set up and executed at Politecnico di Milano. After a hot-wire survey of the isolated stream-wise vortex, the flow was investigated by means of Particle Image Velocimetry (PIV).

2 The test rig

The experimental activity was carried out in the closed-return wind tunnel at Aerodynamic Laboratory of the Dipartimento di Scienze e Tecnologie Aerospaziali (DSTA) of Politecnico di Milano. The wind tunnel has a rectangular test section with 1.5 m height and 1 m width. The maximum wind velocity is 55 m/s with a turbulence level less than 0.1%.

Two NACA 23012 airfoil models with 0.3 m chord were used in the test rig. The upstream model (VG) was still and it was used as a vortex generator, spanning half of the test section width. The second model constitutes the target of the stream-wise vortex and is mechanically jointed to a driving system that makes it to oscillate in pitch around the axis at 25% of the airfoil chord. The oscillating model driving system is composed by a brushless servomotor with a 12:1 gear drive. More details about the description of the pitching airfoil experimental rig can be found in [5, 6].

Figure 1 presents the test layout as well as the reference system used in the present activity (the x-axis corresponds to the test section central axis). The leading edge of the oscillating model is positioned 3.5 c past the trailing edge of the vortex generator model.

The tests considered in the present study were carried out at $U_\infty = 30$ m/s (corresponding to a Reynolds number of $\mathrm{Re} = 6 \times 10^5$ and a Mach number of $\mathrm{Ma} = 0.09$) with the airfoil model pitching at the reduced frequency $k = 0.1$ around the mean angle of attack $\alpha_m = 5°$ or $\alpha_m = 10°$. At the maximum angle of attack ($\alpha = 20°$) the wind tunnel blockage, based on the airfoil projected frontal area, was 6%. The upstream model (the vortex generator) was kept at $\alpha = 10°$.

3 3D Hot-Wire measurements of the isolated vortex

The adopted Hot-Wire (HW) system was based on a tri-axial fiber-film probe (with hree 70 μm diameter nickel-plated quartz fibres) controlled by a constant temperature anemometry unit. The probe was calibrated in laboratory under monitored conditions, with respect to Reynolds

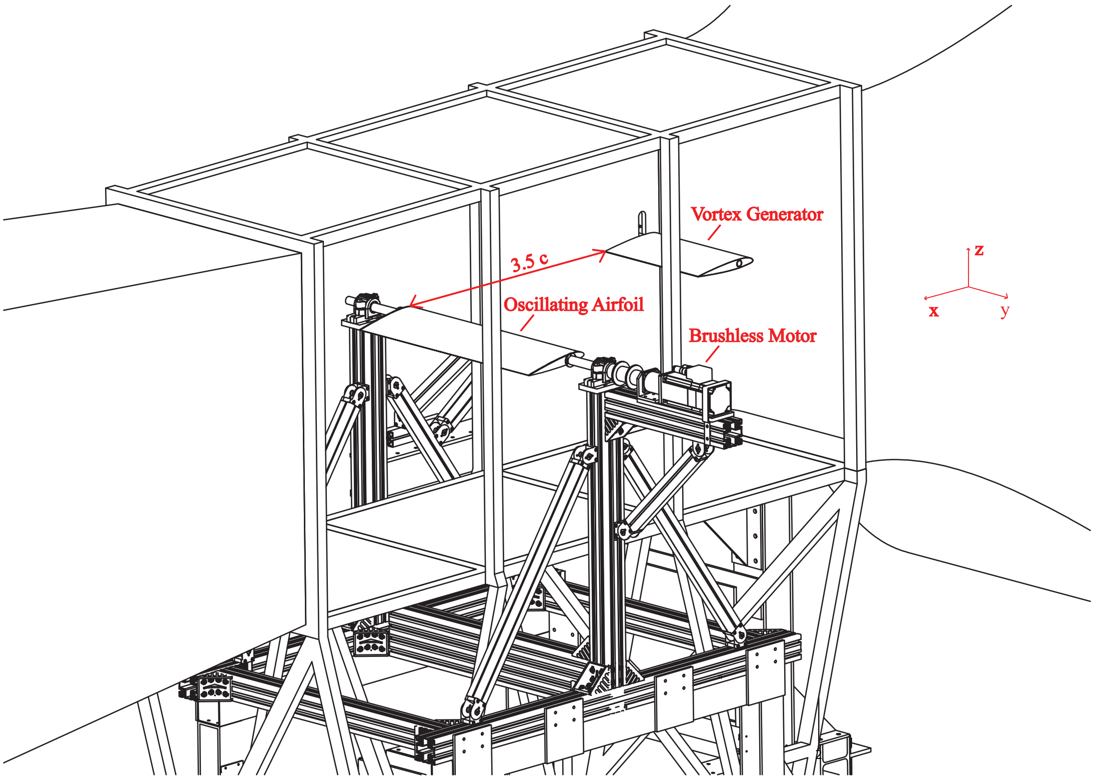

Figure 1: Layout of the BVI test rig.

number and velocity direction. The calibration method took into account the effects of temperature, pressure and humidity in order to extend the calibration itself to the wind tunnel ambient conditions [?]. The HW measurements were carried out without the target airfoil in order to describe the isolated vortex itself. The probe was moved in the y-z plane by means of a dual axis traversing system on a 100 mm × 100 mm measurement window centred on the reference system origin. The velocity time history for each grid point was measured for 15 s with a sampling frequency of 2 kHz. Figure 2 shows a picture of the 3D HW probe set up inside the wind tunnel test section.

Figure 3 shows the results of the 3D HW measurements carried out on the y-z plane with the upstream model at $\alpha = 10°$. In particular, Fig. 3 shows the velocity vector field of the isolated vortex.

A problem affecting the streamwise vortices generated inside a wind-tunnel test chamber is a low-frequency oscillation of the vortex cenerline, called "vortex wandering" [7, 8], that apparently does not affect free-stream wortices. Due to the wandering, the average vortex is more diffused respect to the actual istantaneus one. A statistical investigation on the hot-wire measurements demonstrated that in the present experiment the wandering was very small (see [6] for details).

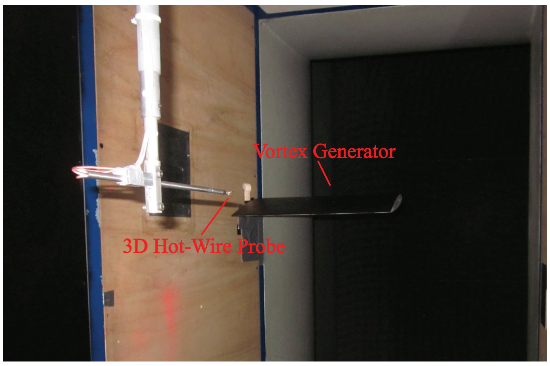

Figure 2: 3D Hot-wire probe set up.

4 PIV measurements

In the present activity 2D flow field surveys were carried out on x-z plane windows at different positions around the oscillating model. The pulsed light sheet was produced by a Nd:Yag

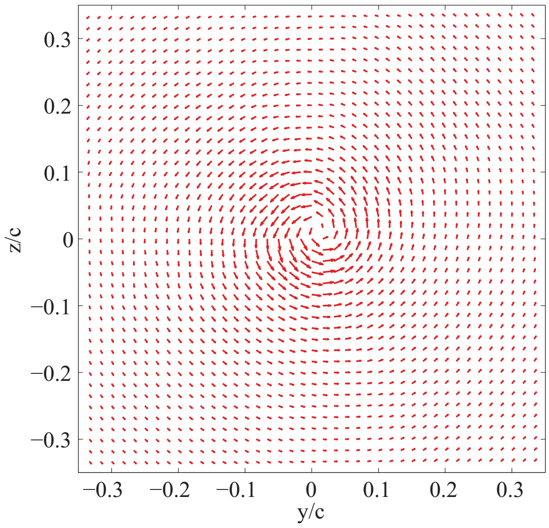

Figure 3: HW velocity vector field of the isolated vortex; VG at $\alpha = 10°$.

double pulsed laser with 200 mJ output energy and a wavelength of 532 nm. The image pairs were acquired by means of a 1MP double shutter CCD camera. The laser and the camera were both fixed to a single axis traversing system. Figure 4 shows a picture of the PIV set up.

Figure 4: PIV set up.

The synchronization of the two laser pulses with the image pairs exposure was controlled by a 6 channels pulse generator. A particle generator with Laskin atomizer nozzles was used for the seeding.

A preliminar test with the isolated vortex was carried out in order to validate the measurements by comparison with the HW results. Figure 5 shows the comparison between the PIV and HW measurements of vortex velocity profile. As it is apparent in the figure, the two techniques demonstrated a quite good agreement.

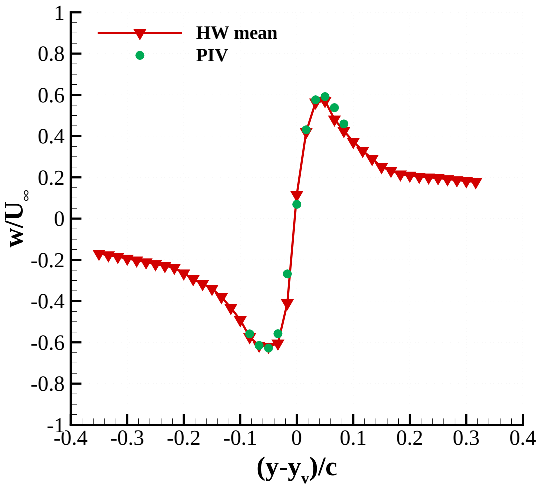

Figure 5: Comparison of the z-component velocity profile measured with HW and PIV at z - $z_v = 0$.

The two oscillation cycles studied in this experiment represent two typical dynamic stall typologies: light dynamic stall regime and deep dynamic stall regime (according to the definition of McCroskey [9]). The pitching cycle with $\alpha_m = 5°$ represents a light dynamic stall regime while the cycle with $\alpha_m = 10°$ represents the deep dynamic stall regime [9].

The tests and pitching cycles parameters are listed in the Tab. 1. As already specified, all the dynamic tests with the oscillating airfoil were carried out at $Re = 6 \cdot 10^5$ and $Ma = 0.09$.

For each test condition (identified by a specific phase of a specific cycle) the position of the upstream model was adjusted in order to get the vortex impact at the target airfoil lead-

α	k	α_m	α_a
$10°$ Upstroke	0.1	$5°$	$10°$
$15°$	0.1	$5°$	$10°$
$10°$ Downstroke	0.1	$5°$	$10°$
$19°$ Upstroke	0.1	$10°$	$10°$

Table 1: PIV test conditions with the oscillating airfoil.

ing edge.

In order to get more resolution, the measurement area was composed by two measurement windows with a small overlapping band between them. The PIV surveys were carried out at two span positions, y - y_v = ±15 mm (corresponding to the vortex viscous core boundaries) and over two adjacent measurement windows (slightly overlapped). For all the BVI tests, the velocity flow fields were obtained by phase averaging the fields obtained by 40 image pairs.

The results are showed from Figure 6 to Figure 9 where the clean flow (no vortex) is compared with the flow produced by the vortex at the two span positions for each tested condition. The figures present the velocity magnitude contours (coloured) together with the two-dimensional streamline patterns (i.e. the streamlines of the in-plane velocity).

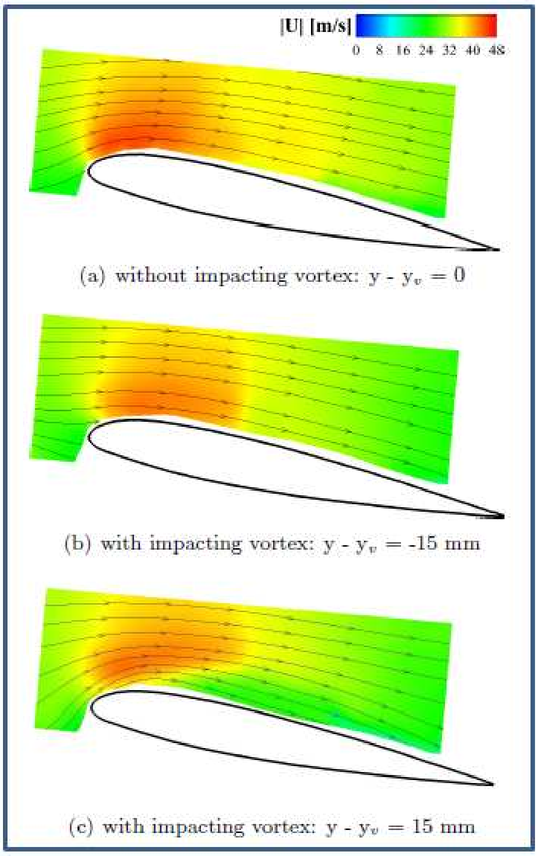

Figure 6: PIV results for the light dynamic stall condition at $\alpha = 10°$ in upstroke.

4.1 Light dynamic stall

The flow on the airfoil upper surface for the clean configuration (without the impinging vortex) is fully attached at $\alpha = 10°$ in upstroke (see Fig. 6a).

On the measurement plane at y - y_v = -15 mm, a strong reduction of the local angle of attack produced by the peak of downward velocity component induced by the vortex can be observed (see in particular the streamlines curvature at the leading edge region in Fig. 6b).Nevertheless, the overall flow behaviour does not show significant modification due the vortex interaction with respect to the clean airfoil configuration.

On the contrary, a strong increase of the local angle of attack can be observed on the measurement plane at y - y_v = 15 mm due to the maximum upward velocity component induced by the vortex (see the conspicuous streamlines deflection at the leading edge region in Fig. 6c). Nevertheless, the flow on the airfoil upper surface does not show a back-flow region.

Considerations similar to the previous test case about the interacting flow field can be deduced from the measurements carried out at y - y_v = -15 mm for the $\alpha = 15°$ condition (see Fig. 7a and b). On the contrary, the apparent distortion of the flow as well as the in-plane streamline patterns illustrated in Fig. 7c for the measurements at y - y_v = 15 mm, show a strong three-dimensionality of the flow-field. In fact, the streamlines arising from the airfoil surface can be explained by a remarkable spanwise velocity component.

The flow survey at $\alpha = 10°$ in downstroke shows still a quite regular behaviour of the flow for the clean airfoil configuration (see Fig. 8a). On the contrary, the impinging vortex on the measurement plane at y - y_v = -15 mm induces an important modification of the flow field field consisting in a general quite lower velocity field over the airfoil upper surface consistent to the

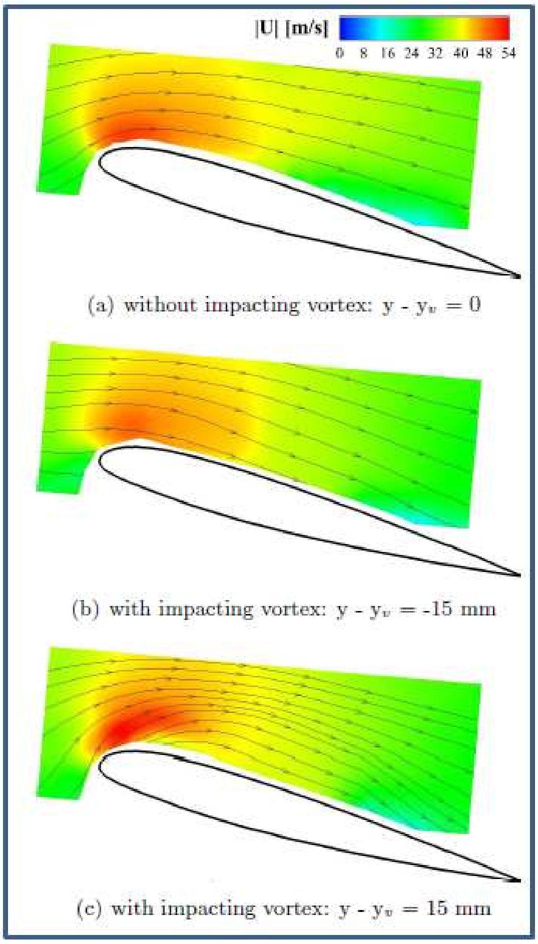

Figure 7: PIV results for the light dynamic stall condition at $\alpha = 15°$ in upstroke.

remarkable effect of the local incidence decrease (see Fig. 8b).

A wide back-flow area on the airfoil upper surface characterised by a large vortical structure can be observed in Fig. 8b) for the measurement plane at y - y_v = 15 mm. The apparent flow field differences observed at $\alpha = 10°$ in downstroke with respect to upstroke case could be explained by the contributory kinematic effect induced by the rapid negative pitching rate of the airfoil that promotes the onset of flow separation in this phase of the pitching cycle [10, 11].

4.2 Deep dynamic stall

For the deep dynanic stall cycle, it was investigated just the $\alpha = 19°$ condition. In this case, as it can be observed in Fig. 9a, the PIV survey show the onset of the flow separation also

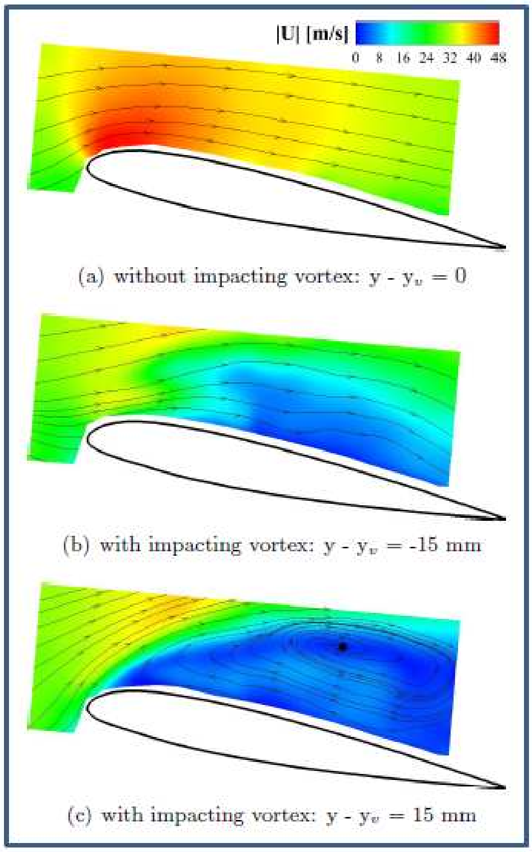

Figure 8: PIV results for the light dynamic stall condition at $\alpha = 10°$ in downstroke.

for the clean airfoil configuration. On the measurement plane at y - y_v = -15 mm the vortex interaction tends to delay the separation at the trailing edge region (see Fig. 9b) consistently to the local decrease of angle of attack induced by the impinging vortex.

On the other hand on the measurement plane at y - y_v = 15 mm a separation bubble at the leading edge region can be observed (see Fig. 9c). Nevertheless, the PIV survey does not show a wide back-flow region that can be expectable due to the upward velocity component induced by the impinging vortex on this plane. In this test case the rapid positive pitching rate produces a contributory camber increase that could explain the measured flow field

4.3 Vortex trajectory

For the light dynamic stall cycle, PIV surveys were carried out over a measurement window centered on the airfoil leading in order to investigate the influence of the airfoil oscillation

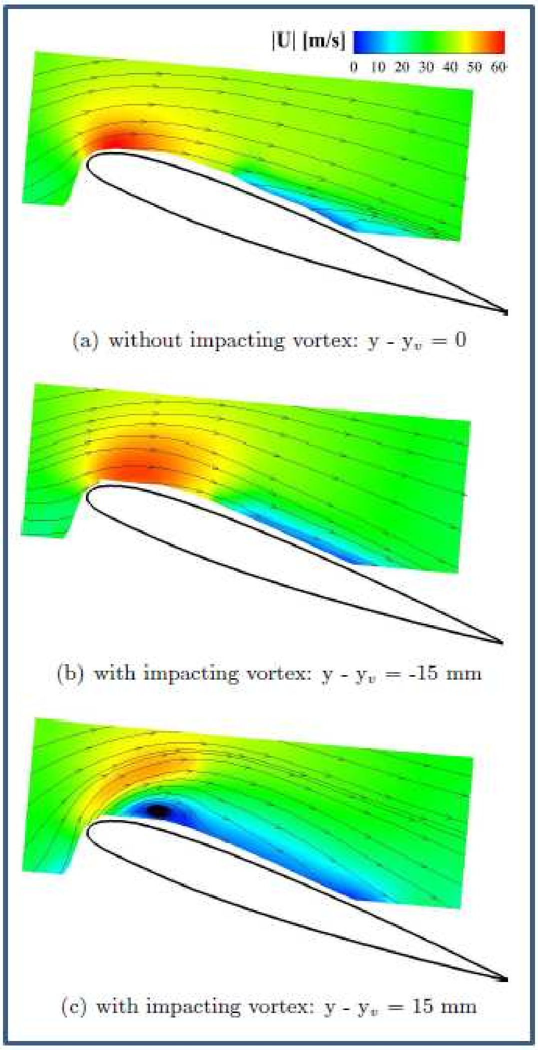

(a) without impacting vortex: y - y_v = 0

(b) with impacting vortex: y - y_v = -15 mm

(c) with impacting vortex: y - y_v = 15 mm

Figure 9: PIV results for the deep dynamic stall condition at $\alpha = 19°$ in upstroke.

on the vortex motion. For this test activity, the upstream model was positioned so that the vortex core impinges the leading edge of the target airfoil at $\alpha = 5°$ in upstroke. Figure 10 shows the contours of the computed divergence of the measured in-plane velocity components. This operator represents, for incompressible flows, represents the variation of the span-wise velocity component in span-wise direction and the change in sign highlights the vortex core attitude.

Figure 10a shows the vortex core impinging the airfoil leading edge at $\alpha = 5°$. In the further part of the upstroke, the induction of the airfoil circulation associated to the lift and the nose-up rotation about its quarter of chord makes the vortex centre-line to be deflected upward as it can be observed in Fig. 10b and c. In fact, the vortex brushes against the airfoil upper surface at $\alpha = 10°$ while it reaches a rather high position over the airfoil in correspondence of $\alpha = 15°$. and 5°. At $\alpha = 10°$ in downstroke motion the vortex centre-line is slightly more deflected upward with respect to the same angle of attack in upstroke (see Fig. 10d), moving downward in the further part of the motion at $\alpha = 5°$ (see Fig. 10 e). When the airfoil reaches $\alpha = 0°$ in downstroke, the vortex core touches again the airfoil upper surface (see Fig. 10f), while in correspondence of the minimum angle of attack of the cycle at $\alpha = -5°$ it goes towards the airfoil lower surface (see Fig. 10g). Then, the start of the upstroke motion make the vortex to arise again as it can be observed at $\alpha = 0°$ in upstroke phase (see Fig. 10h).

5 Conclusions

A dedicated experimental activity showed the effects of a perpendicular vortex impacting on an oscillating airfoil in light and deep dynamic stall conditions. Thanks to the PIV technique a detailed description of the interacting flow over the airfoil was obtained. The experiment allowed to include the effect of airfoil oscillation (that was found to be important).
It has been found that the incidence induced by the vortex (particularly when combined with the downstroke pitching) can produce flow separations. In same conditions these separation regions are so large to be an evidence of local airfoil stall. This is an indication that a perpendicular vortex impact introduce detrimental effects on the blade performance.
The obtained results can also be considered an useful test case to be used as validation benchmark for CFD tools.

Copyright Statement

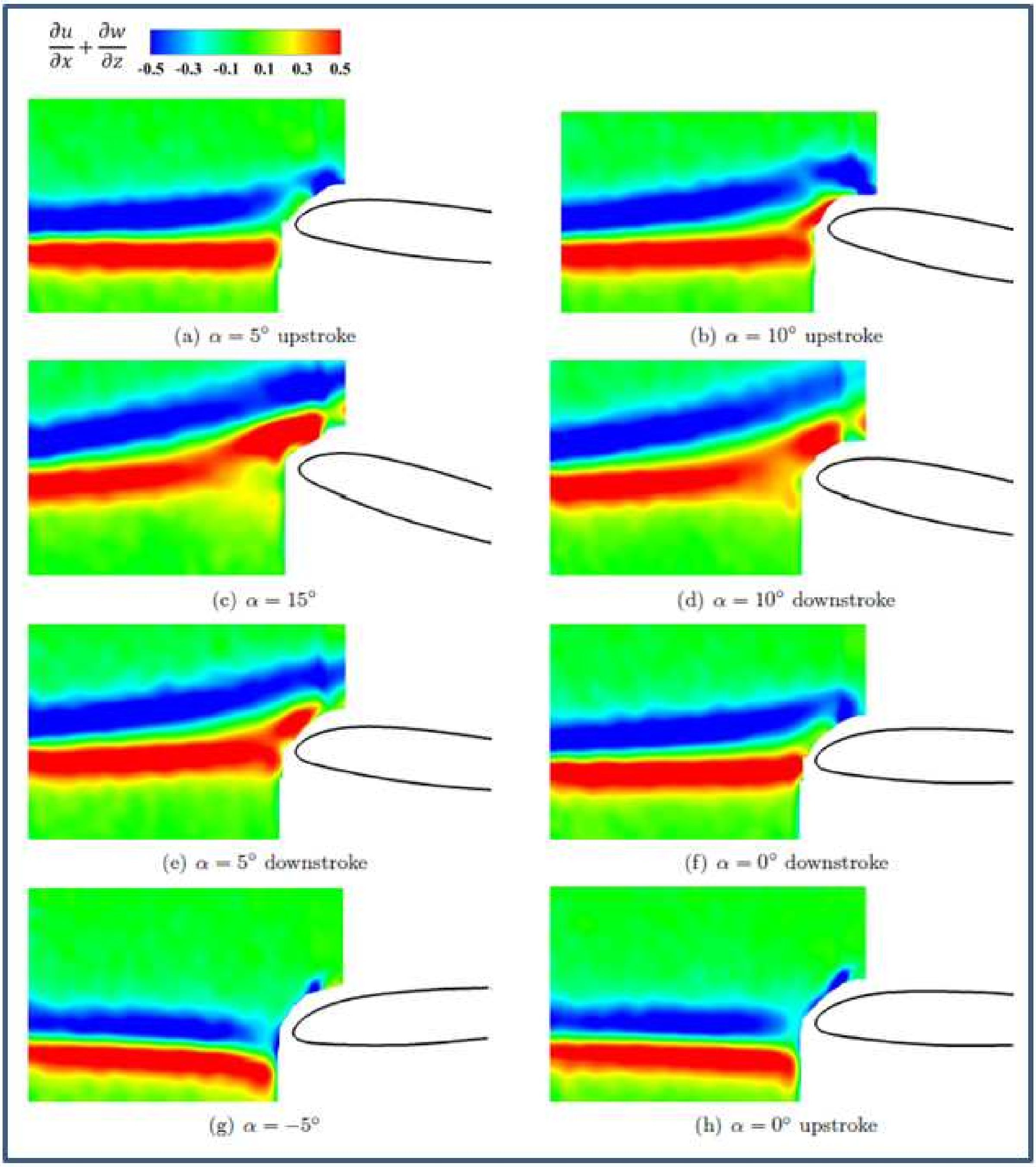

(a) $\alpha = 5°$ upstroke

(b) $\alpha = 10°$ upstroke

(c) $\alpha = 15°$

(d) $\alpha = 10°$ downstroke

(e) $\alpha = 5°$ downstroke

(f) $\alpha = 0°$ downstroke

(g) $\alpha = -5°$

(h) $\alpha = 0°$ upstroke

Figure 10: Trajectory of the vortex for the light dynamic stall condition (contours of the divergence of the in-plane velocity components measured by PIV at z - z_v = 0).

authors confirm that they give permission, or have obtained permission from the copyright holder of this paper, for the publication and distribution of this paper as part of the ERF2013 proceedings or as individual offprints from the proceedings and for inclusion in a freely accessible web-based repository.

References

[1] Y. Yu. Rotor blade-vortex interaction noise, *Progress in Aerospace Sciences*, **36**, 97-115, 2000.

[2] N. Ham. Some Conclusions from an Investigation of Blade-Vortex Interaction, *Jour-*

nal of the American Helicopter Society, **4**, 26-31, 1975.

[3] K.S. Wittmer, W.J. Devenport, M.C. Rife and S.A.L. Glegg. Perpendicular Blade Vortex Interaction, *AIAA Journal*, **33**, 1667-1674, 1995.

[4] K.S. Wittmer and W.J. Devenport. Effects of Perpendicular Blade-Vortex Interaction, Part 1: Turbulence Structure and Development, *AIAA Journal*, **37**, 805-812, 1999.

[5] A. Zanotti, F. Auteri, G. Campanardi and G. Gibertini. An Experimental Set Up for the Study of the Retreating Blade Dynamic Stall, *37th European Rotorcraft Forum*, Gallarate (VA), Italy, 13-15 September 2011.

[6] G. Gibertini, A. Mencarelli and A. Zanotti. Oscillating aerofoil and Perpendicular Vortex Interaction, *Proceedings of the Institution of Mechanical Engineers, Part G: Journal of Aerospace Engineering*, Epub ahead of print 9 April 2013, doi:10.1177/0954410013481154.

[7] W. Devenport, M. Rife, S. Liapis and G. Follin. The structure and development of a wing-tip vortex, *Journal of Fluid Mechanics*, **312**, 67-106, 1996.

[8] G. Iungo, P. Skinner and G. Buresti. Correction of wandering smoothing effects on static measurements of a wing-tip vortex, *Experiments in Fluids*, **46**, 435-452, 2009.

[9] W.J. McCroskey. The Phenomenon of Dynamic Stall, NASA TM 81264, 1981.

[10] J.G. Leishman. Principles of helicopter aerodynamics, Cambridge University Press, 2006.

[11] A. Zanotti and G. Gibertini. Experimental investigation of the dynamic stall phenomenon on a NACA 23012 oscillating airfoil, *Proceedings of the Institution of Mechanical Engineers, Part G: Journal of Aerospace Engineering*, Epub ahead of print 20 July 2012, doi:10.1177/0954410012454100.